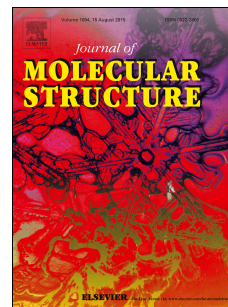


# Accepted Manuscript

4'-(2H-tetrazol-5-yl)-[1,1'-biphenyl]-4-carboxylic acid: Synthetic approaches, single crystal X-ray structures and antimicrobial activity of intermediates

Rodinel Ardeleanu, Andrei Dascălu, Sergiu Shova, Alina Nicolescu, Irina Roșca, Bogdan-Ionel Bratanovici, Vasile Lozan, Gheorghe Roman



PII: S0022-2860(18)30787-7

DOI: [10.1016/j.molstruc.2018.06.086](https://doi.org/10.1016/j.molstruc.2018.06.086)

Reference: MOLSTR 25373

To appear in: *Journal of Molecular Structure*

Received Date: 22 February 2018

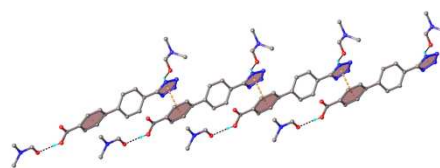
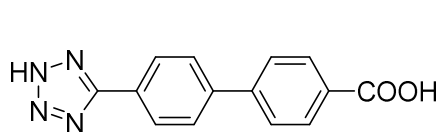
Revised Date: 20 June 2018

Accepted Date: 21 June 2018

Please cite this article as: R. Ardeleanu, A. Dascălu, S. Shova, A. Nicolescu, I. Roșca, B.-I. Bratanovici, V. Lozan, G. Roman, 4'-(2H-tetrazol-5-yl)-[1,1'-biphenyl]-4-carboxylic acid: Synthetic approaches, single crystal X-ray structures and antimicrobial activity of intermediates, *Journal of Molecular Structure* (2018), doi: 10.1016/j.molstruc.2018.06.086.

This is a PDF file of an unedited manuscript that has been accepted for publication. As a service to our customers we are providing this early version of the manuscript. The manuscript will undergo copyediting, typesetting, and review of the resulting proof before it is published in its final form. Please note that during the production process errors may be discovered which could affect the content, and all legal disclaimers that apply to the journal pertain.

## Graphical abstract



ACCEPTED MANUSCRIPT

**4'-(2H-Tetrazol-5-yl)-[1,1'-biphenyl]-4-carboxylic acid: Synthetic approaches, single crystal X-ray structures and antimicrobial activity of intermediates**

Rodinel Ardeleanu<sup>a</sup>, Andrei Dascălu<sup>a</sup>, Sergiu Shova<sup>a</sup>, Alina Nicolescu<sup>a</sup>, Irina Roșca<sup>a</sup>,  
Bogdan-Ionel Bratanovici<sup>a,b</sup>, Vasile Lozan<sup>a,c\*</sup>, Gheorghe Roman<sup>a\*</sup>

<sup>a</sup>*Petru Poni Institute of Macromolecular Chemistry, Iași 700487, Romania*

<sup>b</sup>*Al. I. Cuza University, Faculty of Chemistry, Iași 700506, Romania*

<sup>c</sup>*Institute of Chemistry, Chișinău MD-2028, Republic of Moldova*

**Abstract:** Two synthetic approaches towards 4'-(2H-tetrazol-5-yl)-[1,1'-biphenyl]-4-carboxylic acid, a valuable organic ligand for the preparation of metal-organic frameworks, are reported. The first reaction sequence leading to the target compound comprises the iodination of [1,1'-biphenyl]-4-carboxylic acid, formation of the methyl ester of 4'-iodo-[1,1'-biphenyl]-4-carboxylic acid, nucleophilic substitution of iodine with cyano, ring closure of tetrazole, and hydrolysis of the ester function. The second synthetic pathway starts from 4-bromobenzonitrile, which is converted through Suzuki coupling with 4-carboxyphenylboronic acid into 4'-cyano-[1,1'-biphenyl]-4-carboxylic acid, which in turn leads to the desired compound after ring closure of tetrazole. All of the synthesized compounds have been fully characterized by IR and <sup>1</sup>H- and <sup>13</sup>C-NMR spectroscopy. Single crystal X-ray structures are reported for the target compound and for methyl esters of 4'-iodo-[1,1'-biphenyl]-4-carboxylic acid and 4'-cyano-[1,1'-biphenyl]-4-carboxylic acid. The target compound and the intermediates showed no antimicrobial activity against *Escherichia coli*, *Staphylococcus aureus* and *Candida albicans*.

**Keywords:** Organic ligand; Tetrazole; Multistep synthesis; Single crystal X-ray structure; Antimicrobial activity.

**Corresponding authors:**

Dr. Vasile Lozan

Institute of Chemistry, 3 Academiei Str., Chișinău MD-2028, Republic of Moldova

E-mail: [vasilelozan@gmail.com](mailto:vasilelozan@gmail.com)

Dr. Gheorghe Roman

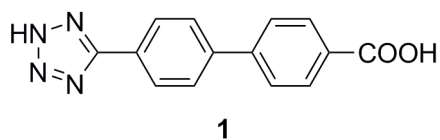
Petru Poni Institute of Macromolecular Chemistry, 41A Aleea Gr. Ghica Vodă, Iași 700487,  
Romania

E-mail: [gheorghe.roman@icmpp.ro](mailto:gheorghe.roman@icmpp.ro)

ACCEPTED MANUSCRIPT

## 1. Introduction

In the last decades, the ongoing search for innovative, high performance compounds in the field of polymers has led to the rapid development of a novel type of materials generically designated as metal-organic frameworks (MOFs). These promising multifunctional materials, which belong to the class of coordination polymers, are compounds that consist of metal ions (or metal clusters) and organic ligands. These two types building units coordinate in a MOF to form one-, two-, or three-dimensional structures that are often porous, which makes MOFs particularly useful for potential industrial applications such as gas storage [1,2], gas separation [3,4], adsorption-driven heat pumps [5], or catalysis [6,7]. Commercially available organic linkers have been so far extensively used for the cheap, rapid and efficient preparation of a large variety of MOFs in large amounts. Nonetheless, the design and preparation of novel organic ligands has started to be employed by numerous research groups with the view to produce hitherto unknown porous coordination polymers with potentially interesting properties. Besides the classical carboxylate ligands, multidentate tetrazolate ligands [8–10] or combined carboxylate-tetrazolate ligands [11–13] have lately emerged as valuable alternatives for the synthesis of novel MOFs. One of the most simple combined carboxylate-tetrazolate ligand is 4'-(2*H*-tetrazol-5-yl)-[1,1'-biphenyl]-4-carboxylic acid **1**, which has been recently used for the synthesis of a cadmium-derived MOF having an intense blue-green photoluminescence emission at room temperature in the solid state [14], for the preparation of a Zn-organic framework for highly selective separation of CO<sub>2</sub> [15], and for obtaining luminescent coordination polymers containing either zinc or cadmium [16]. However, the aforementioned ligand was obtained from 4'-cyano-[1,1'-biphenyl]-4-carboxylic acid using a template reaction in the presence of Cd<sup>2+</sup> in the first study, while the other two articles only mention that the required ligand was purchased from commercial sources. Consequently, there is no available comprehensive report on the synthesis of this valuable ligand from simple starting materials, and there is no structural characterization for the intermediates and the final compound. As a part of our program for the development of novel coordination polymers, the present work aims at correcting this omission by reporting two different approaches for the synthesis of ligand **1**, several X-ray single crystal structures for selected intermediates and for the target compound. In addition, taking into account the status of biphenyl as privileged scaffold in medicinal chemistry [17–19], the investigation of the antimicrobial activity of these compounds has also been undertaken.



## 2. Experimental

### 2.1. Materials and methods

Starting materials and reagents ([1,1'-biphenyl]-4-carboxylic acid **2**, bis[(trifluoroacetoxy)iodo]benzene, 4-bromobenzonitrile **7**, 4-carboxyphenylboronic acid, tetrakis(triphenylphosphine)palladium(0), iodine, copper(I) cyanide, sodium azide, ammonium chloride, anh. potassium carbonate, 36.5% hydrochloric acid, 98% sulfuric acid, sodium hydroxide) were obtained from Alfa Aesar (Ward Hill, MA, USA) and were used without further purification. Most of the solvents (*N,N*-dimethylformamide (DMF), abs. methanol, methanol, chloroform, dioxane, ethanol) were purchased from VWR International (Radnor, PA, USA), only carbon tetrachloride was a product of Chemical Company (Iași, Romania). Mueller–Hinton agar was provided by Merck (Darmstadt, Germany). Melting points were taken on a MEL-TEMP capillary melting point apparatus and are uncorrected. NMR spectra were recorded on a Bruker Avance III 400 instrument operating at 400.1 and 100.6 MHz for  $^1\text{H}$  and  $^{13}\text{C}$  nuclei, respectively, either in  $\text{DMSO-}d_6$  or  $\text{CDCl}_3$ . Chemical shifts are reported in ppm relative to the residual solvent peak ( $^1\text{H}$ : 7.26 ppm and  $^{13}\text{C}$ : 77.01 ppm for  $\text{CDCl}_3$ ;  $^1\text{H}$ : 2.51 ppm and  $^{13}\text{C}$ : 39.47 ppm for  $\text{DMSO-}d_6$ ). Unambiguous 1D NMR signal assignments were made based on 2D NMR homo- and heteronuclear correlations such as H,H-COSY, H,C-HSQC and H,C-HMBC experiments, which were recorded using standard pulse sequences in the version with  $z$ -gradients, as delivered by Bruker with TopSpin 2.1 PL6 spectrometer control and processing software. Fourier Transform-Infrared (FT-IR) spectra were taken on a FT-IR Bruker Vertex 70 spectrophotometer in transmission mode, using KBr pellets. Elemental analysis has been performed on a Vario EL III CHNS analyzer.

### 2.2. Synthesis

**2.2.1. 4'-Iodo-[1,1'-biphenyl]-4-carboxylic acid **3**.** A mixture of [1,1'-biphenyl]-4-carboxylic acid **2** (13.87 g, 70 mmol), bis[(trifluoroacetoxy)iodo]benzene (30.38 g, 70 mmol) and finely ground iodine (17.76 g, 70 mmol) in carbon tetrachloride (180 mL) was stirred at room temperature for 24 h. The resulting solid was filtered, washed with carbon tetrachloride (3×30 mL) and dried under high vacuum to afford the pure product (19.27 g, 85%), mp 315–317 °C (lit. mp 310 °C [20]). FT-IR (ATR),  $1/\nu$  ( $\text{cm}^{-1}$ ): 3107, 2988, 2816, 2673, 2550, 1684, 1607,

1576, 1551, 1516, 1475, 1425, 1394, 1302, 1198, 1177, 1124, 1063, 997, 951, 868, 822, 770, 746, 704, 662, 554, 482, 407.  $^1\text{H-NMR}$  (400 MHz,  $\text{DMSO-}d_6$ ),  $\delta$  (ppm): 7.55 (d, 2H,  $^3J = 12$  Hz, H-2'), 7.79 (d, 2H,  $^3J = 8$  Hz, H-2), 7.86 (d, 2H,  $^3J = 8$  Hz, H-3'), 8.03 (d, 2H,  $^3J = 8$  Hz, H-3), 12.97 (bs, 1H, OH).  $^{13}\text{C-NMR}$  (100 MHz,  $\text{DMSO-}d_6$ ),  $\delta$  (ppm): 95.0 (C-4'), 126.6 (C-2), 129.1 (C-2'), 129.9 (C-4), 130.0 (C-3), 137.8 (C-3'), 138.4 (C-1'), 143.1 (C-1), 167.0 (COOH). *Anal.* Calc. for  $\text{C}_{13}\text{H}_9\text{IO}_2$ : C, 48.17; H, 2.80. Found: C, 48.02; H, 2.72.

**2.2.2. Methyl 4'-iodo-[1,1'-biphenyl]-4-carboxylate 4.** To a suspension of 4'-iodo-[1,1'-biphenyl]-4-carboxylic acid **3** (12 g, 37 mmol) in abs. methanol (300 mL), concentrated sulfuric acid (7 mL) was added dropwise during 1 h. The reaction mixture was heated at reflux temperature for 72 h, and then it was allowed to cool to room temperature. The separated solid was filtered, washed with abs. methanol ( $2 \times 20$  mL), and dried in an oven at 60 °C overnight to give colorless crystals (12.2 g, 97%), mp 192–193 °C (lit. mp 188 °C [20]). FT-IR (ATR),  $1/\nu$  ( $\text{cm}^{-1}$ ): 3456, 2943, 2374, 1780, 1711, 1610, 1576, 1535, 1526, 1516, 1466, 1435, 1379, 1337, 1286, 1198, 1107, 1063, 999, 949, 862, 820, 764, 694, 582, 501, 457.  $^1\text{H-NMR}$  (400 MHz,  $\text{CDCl}_3$ ),  $\delta$  (ppm): 3.94 (s, 3H,  $\text{CH}_3$ ), 7.36 (d, 2H,  $^3J = 8$  Hz, H-2'), 7.62 (d, 2H,  $^3J = 8$  Hz, H-2), 7.80 (d, 2H,  $^3J = 12$  Hz, H-3'), 8.10 (d, 2H,  $^3J = 8$  Hz, H-3).  $^{13}\text{C-NMR}$  (100 MHz,  $\text{CDCl}_3$ ),  $\delta$  (ppm): 52.2 ( $\text{CH}_3$ ), 94.2 (C-4'), 126.8 (C-2), 129.0 (C-2'), 129.3 (C-4), 130.2 (C-3), 138.5 (C-3'), 139.5 (C-1'), 144.4 (C-1), 166.8 (COOMe). *Anal.* Calc. for  $\text{C}_{14}\text{H}_{11}\text{IO}_2$ : C, 49.73; H, 3.28. Found: C, 49.61; H, 3.21.

**2.2.3. Methyl 4'-cyano-[1,1'-biphenyl]-4-carboxylate 5.** A mixture of methyl 4'-iodo-[1,1'-biphenyl]-4-carboxylate **4** (12 g, 35.5 mmol) and  $\text{CuCN}$  (4.76 g, 53.25 mmol) in anh. DMF (170 mL) was heated at 120 °C under argon for 3 d. The cooled reaction mixture was then slowly poured into 1.2 L of distilled water under efficient stirring. The resulting solid was filtered, washed thoroughly with distilled water, and dried in an oven at 105 °C overnight. The dried material was extracted with chloroform (70 mL), and the suspension was filtered. Chloroform was removed under reduced pressure to give a yellowish solid (7.8 g, 93%), mp 143–144 °C. FT-IR (ATR)  $1/\nu$ : 3866, 3744, 3667, 3566, 3366, 3059, 2959, 2374, 2222, 1929, 1724, 1655, 1603, 1564, 1483, 1427, 1281, 1182, 1105, 1007, 957, 833, 768, 721, 696, 652, 563, 517, 451, 372.  $^1\text{H-NMR}$  (400 MHz,  $\text{DMSO-}d_6$ ),  $\delta$  (ppm): 3.90 (s, 3H,  $\text{CH}_3$ ), 7.92 (d, 2H,  $^3J = 8$  Hz, H-2), 7.95–7.99 (m, 4H, H-2' and H-3'), 8.08 (d, 2H,  $^3J = 8$  Hz, H-3).  $^{13}\text{C-NMR}$  (100 MHz,  $\text{DMSO-}d_6$ ),  $\delta$  (ppm): 52.2 ( $\text{CH}_3$ ), 110.9 (C-4'), 118.6 (CN), 127.4 (C-2), 127.9 (C-2'), 129.5 (C-4), 129.8 (C-3), 132.9 (C-3'), 142.6 (C-1), 143.2 (C-1'), 165.8 (COOMe). *Anal.* Calc. for  $\text{C}_{15}\text{H}_{11}\text{NO}_2$ : C, 75.94; H, 4.67; N, 5.90. Found: C, 75.88; H, 4.62; N, 5.83.

**2.2.4. Methyl 4'-(2H-tetrazol-5-yl)-[1,1'-biphenyl]-4-carboxylate 6.** A solution of methyl 4'-cyano-[1,1'-biphenyl]-4-carboxylate **5** (5.35 g, 22.6 mmol), sodium azide (5.53 g, 85 mmol) and ammonium chloride (4.55 g, 85 mmol) in anh. DMF (130 mL) was heated at 120 °C under argon for 3 d. The cooled reaction mixture was then slowly poured into 350 mL of distilled water under efficient stirring. The separated solid material was filtered, washed with distilled water (3×50 mL), and dried in an oven at 105 °C overnight to give colorless crystals (5.75 g, 91%), mp 263–265 °C. FT-IR (ATR)  $1/\nu$ : 3476, 3074, 2928, 2853, 2679, 2552, 1680, 1609, 1578, 1522, 1491, 1423, 1321, 1300, 1180, 1121, 1086, 1030, 997, 922, 899, 876, 833, 775, 746, 698, 675, 552, 498.  $^1\text{H-NMR}$  (400 MHz, DMSO- $d_6$ ),  $\delta$  (ppm): 3.88 (s, 3H, CH<sub>3</sub>), 7.89 (d, 2H,  $^3J = 8$  Hz, H-2), 7.96 (d, 2H,  $^3J = 8$  Hz, H-2'), 8.05 (d, 2H,  $^3J = 8$  Hz, H-3), 8.16 (d, 2H,  $^3J = 8$  Hz, H-3').  $^{13}\text{C-NMR}$  (100 MHz, DMSO- $d_6$ ),  $\delta$  (ppm): 52.1 (CH<sub>3</sub>), 124.1 (C-4'), 127.0 (C-2), 127.6 (C-3'), 127.9 (C-2'), 129.0 (C-4), 129.8 (C-3), 141.1 (C-1'), 143.3 (C-1), 155.1 (C=N), 165.9 (COOMe). *Anal.* Calc. for C<sub>15</sub>H<sub>12</sub>N<sub>4</sub>O<sub>2</sub>: C, 64.28; H, 4.32; N, 19.99. Found: C, 64.18; H, 4.28; N, 19.61.

**2.2.5. 4'-(2H-Tetrazol-5-yl)-[1,1'-biphenyl]-4-carboxylic acid 1.** A mixture of methyl 4'-(2H-tetrazol-5-yl)-[1,1'-biphenyl]-4-carboxylate **6** (3.55 g, 12.67 mmol), NaOH (2.53 g) and distilled water (250 mL) were heated at 90 °C until a clear solution was obtained. The cooled solution was gradually treated with 17% HCl until pH 1-2. The resulting solid was filtered and thoroughly washed with distilled water until the pH of the washings was neutral. The wet material was stirred with acetone (70 mL), filtered and dried in an oven at 60 °C overnight to afford a colorless solid (3.35 g, 95%), which was recrystallized from DMF to give colorless crystals, mp 316–318 °C. FT-IR (ATR)  $1/\nu$ : 3487, 2930, 1676, 1612, 1568, 1518, 1491, 1427, 1391, 1294, 1182, 1107, 1067, 995, 926, 876, 835, 779, 744, 698, 669, 554, 503, 463, 413.  $^1\text{H-NMR}$  (400 MHz, DMSO- $d_6$ ),  $\delta$  (ppm): 7.92 (d, 2H,  $^3J = 8$  Hz, H-2), 8.01 (d, 2H,  $^3J = 8$  Hz, H-2'), 8.07 (d, 2H,  $^3J = 8$  Hz, H-3), 8.13 (d, 2H,  $^3J = 8$  Hz, H-3'), 13.07 (s, 1H, OH), 16.97 (bs, 1H, NH).  $^{13}\text{C-NMR}$  (100 MHz, DMSO- $d_6$ ),  $\delta$  (ppm): 123.9 (C-4'), 127.0 (C-2), 127.6 (C-3'), 127.9 (C-2'), 130.0 (C-3), 130.3 (C-4), 141.5 (C-1'), 143.0 (C-1), 155.1 (C=N), 167.0 (COOH). *Anal.* Calc. for C<sub>14</sub>H<sub>10</sub>N<sub>4</sub>O<sub>2</sub>·2DMF: C, 58.24; H, 5.87; N, 20.38. Found: C, 58.12; H, 5.77; N, 20.31.

**2.2.6. 4'-Cyano-[1,1'-biphenyl]-4-carboxylic acid 8.** To a solution of 4-bromobenzonitrile **7** (3.1 g, 17 mmol) in dioxane (100 mL) was added a solution of 4-carboxyphenylboronic acid (4.15 g, 25 mmol) in ethanol (30 mL), followed by a solution of anh. potassium carbonate (17.39 g, 126 mmol) in deionized water (30 mL). The reaction mixture was degassed by passing a stream of argon through it for 20 min. After tetrakis(triphenylphosphine)palladium

(0.589 g, 0.51 mmol, 3% molar) had been added, the reaction flask was fitted with a condenser and immersed in an oil bath. The reaction mixture was stirred at 85 °C for 24 h, and then it was cooled to room temperature before deionized water (100 mL) was added. The mixture was stirred at room temperature for 1 h, and then it was filtered to remove the insoluble materials. The solution was treated with 10% HCl until pH 4 under efficient stirring to give a colorless precipitate, which was collected by filtration, thoroughly washed with water (300 mL), and dried under reduced pressure at 60 °C. Recrystallization of the solid from DMF afforded colorless plates (2.6 g, 78%), mp 273–275 °C. FT-IR (ATR)  $1/\nu$ : 2669, 2550, 2374, 2222, 1803, 1686, 1603, 1568, 1425, 1296, 1182, 1119, 1007, 932, 872, 827, 770, 698, 555, 515.  $^1\text{H-NMR}$  (400 MHz,  $\text{DMSO-}d_6$ ),  $\delta$  (ppm): 7.88 (d, 2H,  $^3J = 8$  Hz, H-2), 7.93–7.98 (m, 4H, H-2' and H-3'), 8.06 (d, 2H,  $^3J = 8$  Hz, H-3), 13.12 (bs, 1H, OH).  $^{13}\text{C-NMR}$  (100 MHz,  $\text{DMSO-}d_6$ ),  $\delta$  (ppm): 110.8 (C-4'), 118.7 (CN), 127.3 (C-2), 127.9 (C-2'), 130.1 (C-3), 130.8 (C-4), 132.9 (C-3'), 142.3 (C-1), 143.5 (C-1'), 167.0 (COOH). *Anal.* Calc. for  $\text{C}_{14}\text{H}_9\text{NO}_2$ : C, 75.33; H, 4.06; N, 6.27. Found: C, 75.22; H, 3.98; N, 6.20.

**2.2.7. 4'-(2H-Tetrazol-5-yl)-[1,1'-biphenyl]-4-carboxylic acid **1**.** A mixture of 4'-cyano-[1,1'-biphenyl]-4-carboxylic acid **8** (2 g, 8.95 mmol), sodium azide (1.5 g, 23.07 mmol) and ammonium chloride (1.24 g, 23.1 mmol) in DMF (40 mL) was stirred at 120 °C for 72 h. The reaction mixture was cooled to room temperature and poured with efficient stirring into deionized water (300 mL). The solid material was collected by filtration, washed with deionized water (150 mL), and dried under reduced pressure at 60 °C. Recrystallization from DMF afforded colorless crystals (1.9 g, 79%), mp 317–319 °C. The IR,  $^1\text{H}$ - and  $^{13}\text{C}$ -NMR spectra of this compound were identical to those recorded for compound **1** obtained through the other synthetic route.

### 2.3. X-ray crystallography

X-ray diffraction measurements for **1** and **5** were carried out with an Oxford-Diffraction XCALIBUR E CCD diffractometer equipped with graphite-monochromated  $\text{MoK}\alpha$  radiation. Single crystals were positioned at 40 mm from the detector and 155, and 242 frames were measured each for 25, and 5 s over  $1^\circ$  scan width for **1** and **5**, respectively. Intensity data for **4** were collected with Oxford Diffraction SuperNova diffractometer using hi-flux micro-focus Nova  $\text{CuK}\alpha$  radiation. The single crystal was positioned at 47 mm from the detector and 452 frames were measured each for 5 s over  $1^\circ$  scan width. The unit cell determination and data integration were carried out using the CrysAlis package of Oxford Diffraction [21]. The structures were solved by direct methods using Olex2 [22] software with

the SHELXS [23] and refined by full-matrix least-squares on  $F^2$  with SHELXL-97 [23] using an anisotropic model for non-hydrogen atoms. All hydrogen atoms were introduced in idealized positions ( $d_{\text{CH}} = 0.96 \text{ \AA}$ ) using the riding model with their isotropic displacement parameters fixed at 120% of their riding atom. Positions of hydrogen atoms for the O-H and N-H groups were located on electron density difference map and refined accounting for the hydrogen bonds parameters. The molecular plots were obtained using the Olex2 program. The crystallographic data and refinement details are quoted in Table 1, while bond lengths are summarized in Table S1 (see Supplementary Material). CCDC-1822343 (**1**·**2DMF**), CCDC-1822346 (**4**) and CCDC-1822342 (**5**) contain the supplementary crystallographic data for this contribution.

**Table 1.** Crystallographic data, details of data collection and structure refinement parameters for compounds **1**·**2DMF**, **4** and **5**.

Compound	<b>1</b> · <b>2DMF</b>	<b>4</b>	<b>5</b>
Empirical formula	$\text{C}_{20}\text{H}_{24}\text{N}_6\text{O}_4$	$\text{C}_{14}\text{H}_{14}\text{INO}$	$\text{C}_{30}\text{H}_{22}\text{N}_2\text{O}_4$
Formula weight	412.45	339.16	474.50
Temperature/K	200	293(2)	293(2)
Crystal system	monoclinic	orthorhombic	monoclinic
Space group	$P2_1/n$	$Pca2_1$	$Pc$
$a/\text{\AA}$	11.9398(12)	6.0538(5)	3.91242(17)
$b/\text{\AA}$	8.1451(7)	7.3253(6)	20.4050(8)
$c/\text{\AA}$	21.943(2)	27.8702(16)	15.2981(5)
$\alpha^\circ$	90.00	90.00	90.00
$\beta^\circ$	104.273(11)	90.00	97.002(4)
$\gamma^\circ$	90.00	90.00	90.00
$V/\text{\AA}^3$	2068.1(4)	1235.91(16)	1212.18(9)
$Z$	4	4	2
$D_{\text{calc}}/\text{mg}/\text{mm}^3$	1.325	1.823	1.300
$\mu/\text{mm}^{-1}$	0.095	2.574	0.087
Crystal size/ $\text{mm}^3$	$0.3 \times 0.2 \times 0.2$	$0.25 \times 0.15 \times 0.02$	$0.35 \times 0.3 \times 0.25$
$\theta_{\text{min}}, \theta_{\text{max}}(^{\circ})$	3.56 to 50.04	6.28 to 50.04	4 to 50.06
Reflections collected	8278	7825	14747
Independent reflections	3655 [ $R_{\text{int}} = 0.0244$ ]	2146 [ $R_{\text{int}} = 0.0494$ ]	4301 [ $R_{\text{int}} = 0.0275$ ]
Dt/restraints/parameters	3655/0/276	2146/1/155	4301/2/327
GOF <sup>c</sup>	1.033	1.057	1.043
$R_1(I > 2\sigma(I))$	0.0490	0.0364	0.0529
$wR_2^b(\text{all dt})$	0.1146	0.0724	0.1428
Largest diff. peak/hole/ $e \text{ \AA}^{-3}$	0.19/-0.18	0.64/-0.61	0.26/-0.15

$R_1 = \Sigma||F_o| - |F_c||/\Sigma|F_o|$ . <sup>b</sup> $wR_2 = \{\Sigma[w(F_o^2 - F_c^2)^2]/\Sigma[w(F_o^2)^2]\}^{1/2}$ . <sup>c</sup> GOF =  $\{\Sigma[w(F_o^2 - F_c^2)^2]/(n-p)\}^{1/2}$ , where  $n$  is the number of reflections and  $p$  is the total number of parameters refined

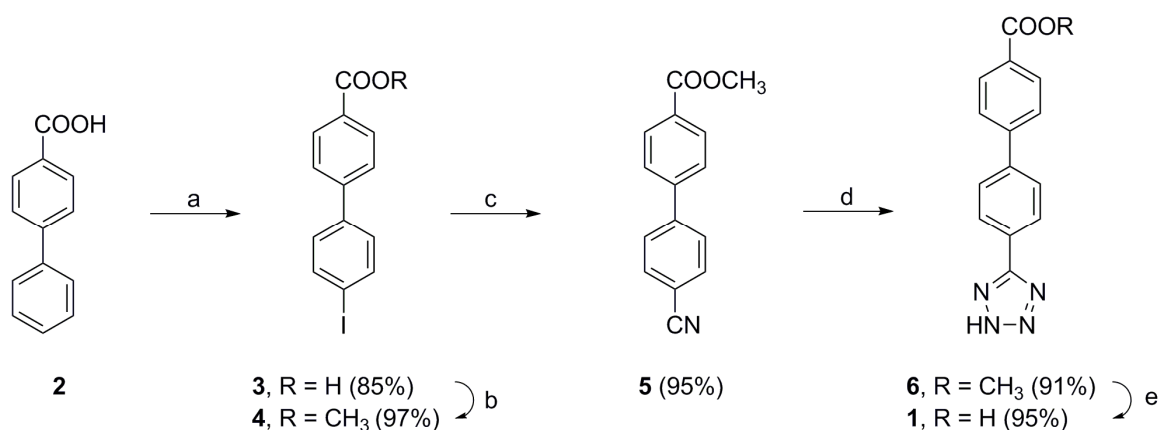
## 2.4. Biological activity

*In vitro* antimicrobial susceptibility of the target compound **1** and of intermediates **3–6** was evaluated using the guidelines of EUCAST [24]. The three different reference strains used in this study were *E. coli* ATCC25922, *S. aureus* ATCC25923 and *C. albicans* ATCC10231. The tests were performed on unsupplemented Mueller–Hinton agar, which was dispersed in Petri dishes in an even layer of 4.0 mm with a maximum variation of  $\pm 0.5$  mm. The inoculum suspension has been prepared by adjusting its density to the density of a McFarland 0.5 standard by addition of 0.85% NaCl w/v in water or more organisms, to achieve a suspension containing  $1 \times 10^8$  CFU/mL for all microorganisms. From each compound to be tested, a stock solution containing 5 mg/mL was prepared by dissolving the tested compounds in dimethylsulfoxide. Each compound has been tested at six different concentrations. The solutions of the tested compounds were obtained by diluting the stock solutions, with the view to reach final concentrations within the range of 0.156–5 mg/mL. After the application of the tested compounds, the plates had been incubated at  $36 \text{ }^\circ\text{C} \pm 1^\circ\text{C}$  for 24 h. After incubation, the diameters of inhibition zones were measured.

### 3. Results and discussion

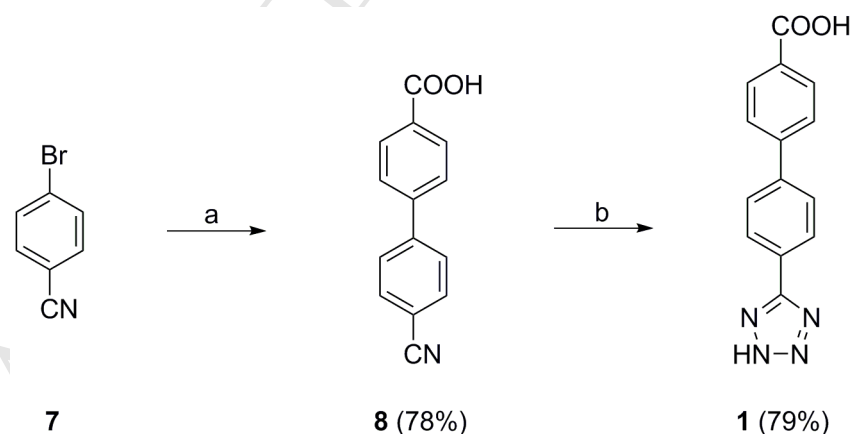
#### 3.1. Chemistry

Using commercially available, affordable reagents, two synthetic approaches have been designed for the preparation of the desired ligand **1**. The first approach employs as starting material a compound having a biphenyl core that is appropriately substituted, whereas the strategy devised for the second approach involves the construction of the biphenyl core from suitable substituted benzene derivatives via a Suzuki–Miyaura cross-coupling reaction. The reaction sequence leading to the target compound **1** through the first approach is given in Scheme 1. Starting from [1,1'-biphenyl]-4-carboxylic acid **2**, intermediate acid **3** is obtained through nuclear iodination using a procedure previously reported in literature [20]. In the next step, intermediate acid **3** is converted into the corresponding methyl ester **4**, which, in turn, is subjected to the replacement of iodine with a nitrile group in a typical a Rosemund–von Braun reaction [25] to afford intermediate **5**. The formation of the tetrazole ring in intermediate **6** was accomplished through a [3+2] dipolar cycloaddition between the nitrile **5** and sodium azide in the presence of ammonium chloride [26]. An initial attempt to conduct the cycloaddition in the presence of anhydrous  $\text{ZnCl}_2$ , as previously reported [27], led to a product containing traces of zinc, whose complete removal proved to be very difficult. Finally, the base-catalyzed hydrolysis of tetrazole–ester **6** afforded the target compound **1** with a very good total yield of 68% in 5 steps and without chromatographic separation.



**Scheme 1.** Synthesis of 4'-(2*H*-tetrazol-5-yl)-[1,1'-biphenyl]-4-carboxylic acid **1**. Reagents and conditions: a) bis[(trifluoroacetoxy)iodo]benzene, I<sub>2</sub>, CCl<sub>4</sub>, rt, 24 h; b) abs. CH<sub>3</sub>OH, conc. H<sub>2</sub>SO<sub>4</sub>, reflux, 72 h; c) CuCN, anh. DMF, 120 °C, 72 h; d) NaN<sub>3</sub>, NH<sub>4</sub>Cl, anh. DMF, 120 °C, 72 h; e) aq. NaOH, 90 °C, several hours.

The second approach towards the preparation of compound **1** is a more straightforward, two-step synthetic strategy, but, compared to the first approach, it requires the use of relatively expensive reagents, namely a boronic acid and a palladium-based catalyst. Thus, in the first step of the reaction sequence, 4-bromobenzonitrile **7** was subjected to a Suzuki-Miyaura cross-coupling reaction with 4-carboxyphenylboronic acid in the presence of tetrakis(triphenylphosphine)palladium(0), then, in the second stage, the intermediate carboxylic acid **8** underwent a [3+2] dipolar cycloaddition with sodium azide in the presence of ammonium chloride leading to the formation of the tetrazole ring (Scheme 2).



**Scheme 2.** Alternative synthesis of 4'-(2*H*-tetrazol-5-yl)-[1,1'-biphenyl]-4-carboxylic acid **1**. Reagents and conditions: a) 4-carboxyphenylboronic acid, K<sub>2</sub>CO<sub>3</sub>, Pd[P(C<sub>6</sub>H<sub>5</sub>)<sub>3</sub>]<sub>4</sub>, dioxane–ethanol–water, 85 °C, 24 h; b) NaN<sub>3</sub>, NH<sub>4</sub>Cl, DMF, 120 °C, 72 h.

The palladium-catalyzed cross-coupling reaction proceeds smoothly even without the use of expensive Schlenk glassware, as long as air is thoroughly excluded from the reaction mixture,

and it could be upscaled to easily and steadily provided batches of several grams of intermediate **8** in a single experiment. With its 62% global yield, this second approach towards the preparation of the target compound **1** provides a valuable alternative to the first synthetic strategy described previously in this study.

### 3.2. IR spectroscopy

All of the synthesized compounds have been structurally characterized using FT-IR spectroscopy (see Supplementary Material). Thus, close comparison of the FT-IR spectra of acid **3** and ester **4** confirmed the conversion of the former into the latter through the shift of the band associated with the vibration of the double bond of the carbonyl group from 1684  $\text{cm}^{-1}$  in acid **3** to 1711  $\text{cm}^{-1}$  in ester **4**. Replacement of iodine in ester **4** with the nitrile group in ester **5** was proven by the identification of the characteristic band for nitriles at 2222  $\text{cm}^{-1}$  in the FT-IR spectrum of compound **5**, while the value of wavelength number recorded for the vibration of the carbonyl bond in ester **5** was 1724  $\text{cm}^{-1}$ . The absence in the FT-IR spectrum of tetrazole-ester **6** of the absorption band associated with the nitrile group confirms the success of the cycloaddition reaction and the formation of the tetrazole ring. The presence of the absorption band at 1680  $\text{cm}^{-1}$  in the FT-IR spectrum of the target compound **1**, correlated with the disappearance of the absorption band usually associated with the carbonyl vibration of the ester function, is suggestive for the hydrolysis of ester **6** to acid **1**. As for intermediate **8**, the absorption band for the carbonyl vibration in carboxylic acids can be identified at 1686  $\text{cm}^{-1}$  in its FT-IR spectrum, while the absorption band due to the stretching of the triple bond in nitriles is found at 2222  $\text{cm}^{-1}$ .

### 3.3. NMR spectroscopy

The structure of the synthesized products was also investigated using NMR spectroscopy. As a general remark, all the compounds reported in this study feature a biphenyl moiety in their structure, the only difference between compounds **1**, **3**, **4**, **5** and **6** resides in the nature of the substituents attached at positions 4 and 4' of the biphenyl ring system. Therefore, in the  $^1\text{H}$ -NMR spectra of these compounds (see Supplementary Material), the aromatic protons in the 4,4'-disubstituted biphenyl appear in the region 6-8 ppm as four doublets presenting a "roof effect", which is characteristic for *para*-disubstitution. The exact chemical shifts values depend on the type of the substituents in each of the compounds **1** and **3-6**. In the  $^{13}\text{C}$ -NMR spectrum of these compounds, the four signals for the CH groups in the 4,4'-disubstituted biphenyl moiety are noticeable in the 125-138 ppm range, while the

chemical shifts values for the quaternary carbons depend heavily on the type of the substituents attached to them. Specifically, the aromatic protons in intermediate **3** appear in the proton spectrum of this compound as four doublets in the region 7.53–8.04 ppm, while the hydroxyl proton is associated with the very broad signal centered at 12.97 ppm. In the  $^{13}\text{C}$ -NMR spectrum of **3**, a signal corresponding to an aromatic quaternary carbon atom is detectable at 95 ppm, which is outside the usual range for aromatic carbon atoms. As this shielding effect is characteristic for elements with many polarizable electrons, such as iodine, this observation provides the necessary confirmation for the presence of iodine in the structure of compound **3**. Next, the presence of methyl ester function in intermediate **4** was associated with the intense singlet integrating for three protons at 3.94 ppm in the proton spectrum of this compound, while the absence in the spectrum of the broad signal assigned to the proton in the carboxyl function in carboxylic acid **3** offered further proof for the conversion of this group into an ester group. In addition, the signal at 52.2 ppm in the  $^{13}\text{C}$ -NMR spectrum of ester **4** could be assigned to the carbon atom in the methyl group. The introduction of nitrile group in the structure of ester **5** induces only a minor downfield shift of 0.6 ppm for the protons at C-2' of the biphenyl ring system compared to the values of the chemical shift for the same protons in ester **4**. However, comparison of the  $^{13}\text{C}$ -NMR spectra of esters **4** and **5** reveals a few major changes that are brought about by the presence of the nitrile group in the structure of ester **5**. First, the carbon atom of the nitrile group was assigned the new signal at 118.6 ppm, which typically appears in that region. Second, the chemical shift value (110.9 ppm) for the quaternary carbon atom C-4' onto which the nitrile function is attached in ester **5** shifted downfield compared to the value recorded for the same protons in 4'-iodo derivative **4**. This shift is usually caused by the  $\pi$ -electron deshielding and polar inductive effects of the cyano group [28, 29]. In the  $^1\text{H}$ -NMR spectrum of compound **6**, the presence of the tetrazole ring induces a downfield shift of 1.0 ppm for the protons at position 3' relative to the value recorded for the same protons in intermediate **5**. The signal for the proton of the tetrazole ring in tetrazole–ester **6** is very broad, and partially overlaps the four signals associated with the protons in the biphenyl moiety. The peak at 118.6 ppm, previously assigned to the carbon atom in the nitrile group is absent in the  $^{13}\text{C}$ -NMR spectrum of tetrazole–ester **6**, and a new broad signal appears at 155.1 ppm. From the bidimensional H,C-HMBC spectrum, this new signal was assigned to the quaternary carbon from the tetrazole ring. The chemical shift value for the quaternary carbon atom C-4' linked to the tetrazole ring is shifted downfield (124.1 ppm) compared to value for the same carbon atom in ester **5** (110.9 ppm), while an upfield shift is observed for C-3'. As a result of the hydrolysis of ester **6**, a new broad signal, typical

for the proton of the carboxyl group, is observed at 13.07 ppm in the  $^1\text{H}$ -NMR spectrum of the target compound **1**. Also, the broad singlet appearing in this downfield region at 16.97 ppm was assigned to the proton of the tetrazole ring.  $^{13}\text{C}$ -NMR spectrum of carboxylic acid **1** is very similar to the carbon spectrum of its methyl ester **6**, with the exception of the peak at 52.1 ppm assigned to the carbon atom in the methyl ester function, which is now absent. In the case of intermediate **8**, the presence of group of signals in the aromatic region of the proton spectrum that integrates for eight protons is indicative for the presence of the biphenyl ring system in the structure of compound **8**. In addition, the broad signal centered at 13.12 ppm, characteristic for the proton of the carboxyl group, confirms the success of the Suzuki coupling. Also, the presence of the nitrile and carboxyl groups in the structure of intermediate **8** is corroborated by the peaks at 118.7 ppm and 167.0 ppm, respectively.

### 3.4. Crystal structure of compounds **1**, **4** and **5**

The solid state structures of the target compound **1** and intermediates **4** and **5** have been determined by single crystal X-ray diffraction method. Crystals of the target compound **1** that were suitable for X ray diffraction studies have been obtained by slowly cooling a concentrated solution of this compound in hot DMF. In the case of compounds **4** and **5**, X ray quality single crystals were obtained from their solutions in methanol and chloroform, respectively, using the slow evaporation technique. All these compounds exhibit a molecular crystal structure comprising neutral entities, as showing in Figures 1, 2 and 3, respectively. The bond distances and angles are summarized in Table S1 (see Supplementary Material). Compounds **4** and **5** crystallize without any solvate molecules, while compound **1** crystallizes with DMF molecules in 1:2 ratio. The molecule of **1** exhibits a planar configuration, which is however broken by the rotation of the C8-C12 phenyl ring at  $17.464(3)^\circ$  to the plane formed by the rest of the atoms. Compound **1** and both solvate DMF molecules are associated via hydrogen bonding where the N-H and O-H functional groups act as donors of protons (Figure 1). The molecule of **4** is essentially planar within 0.11 Å, with the maximum deviation at 0.22 Å observed for the methyl group. The crystal of **5** shows the presence of two discrete chemically equivalent but crystallographic independent molecules in the asymmetric part of the cell (denoted as **A** and **B**). Due to their similarity, only one of the independent molecules will be characterized in details below. The molecule of **5** features a non-planar structure with the dihedral angle between two aromatic rings of  $38.51$  and  $37.69^\circ$  for **A** and **B** molecules, respectively.

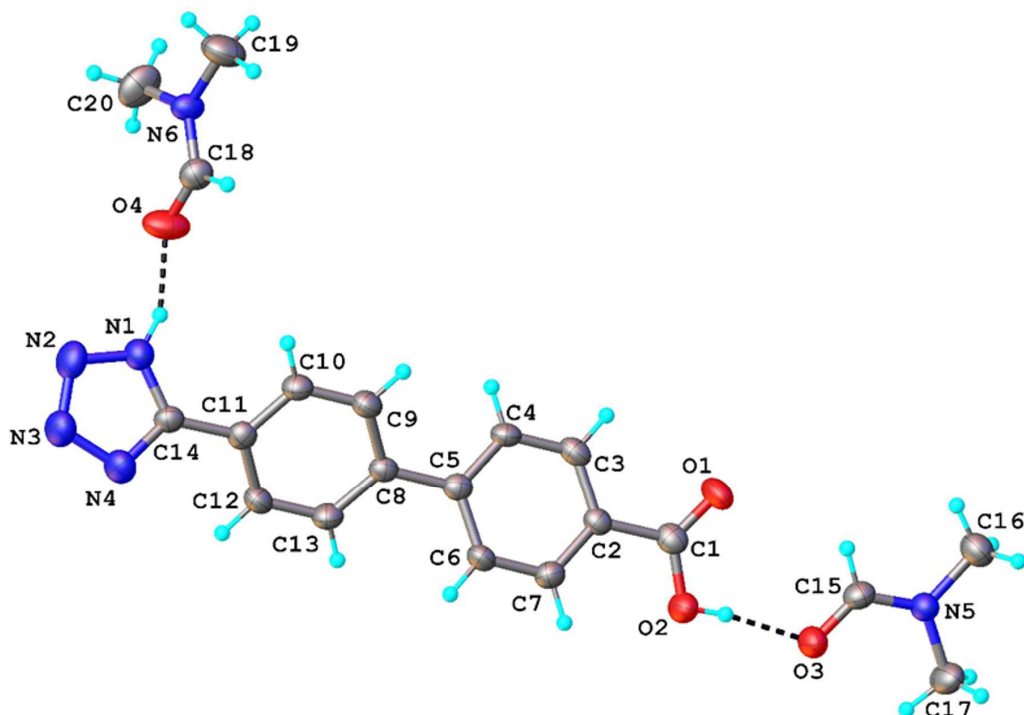


**Figure 1.** View of the asymmetric part in the crystal **1·2DMF** with atom numbering and thermal ellipsoids at 50% probability level. H-bonds are drawn in black dashed lines. H-bonds parameters: O2-H $\cdots$ O3 [O2-H 0.82 Å, H $\cdots$ O3 1.75 Å, O2 $\cdots$ O3 2.568(2) Å,  $\angle$ O2HO3 171.8°]; N1-H $\cdots$ O4 [N1-H 0.82 Å, H $\cdots$ O4 1.84 Å, N1 $\cdots$ O4 2.646(2) Å,  $\angle$ N1HO4 155.5°].

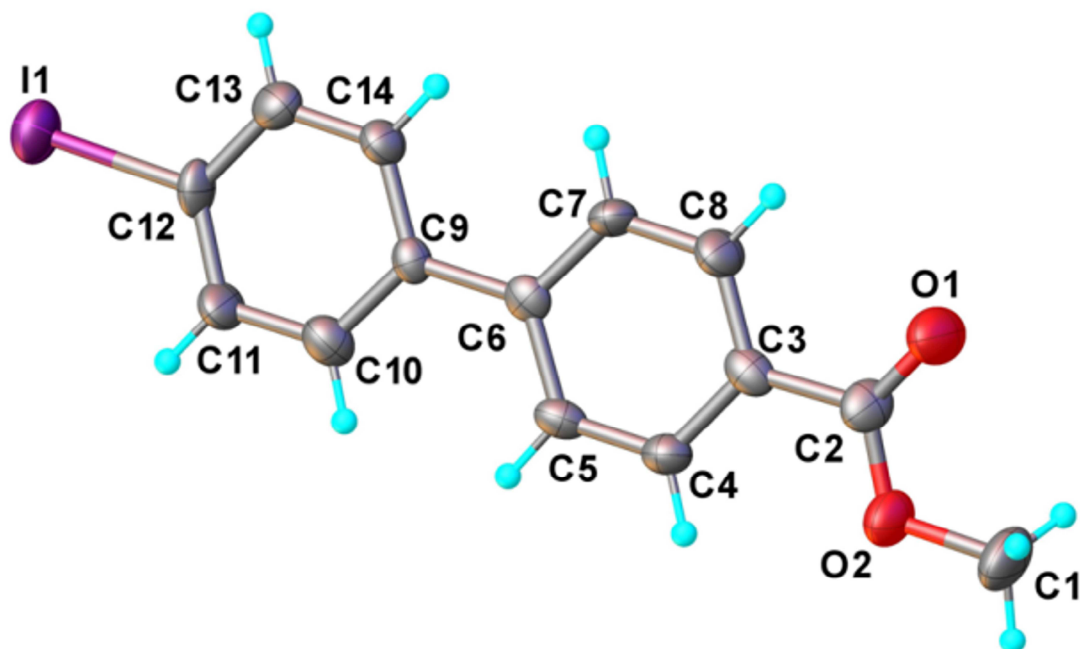


**Figure 2.** X-ray molecular structure of **4** with atom numbering and thermal ellipsoids at 50% probability level.

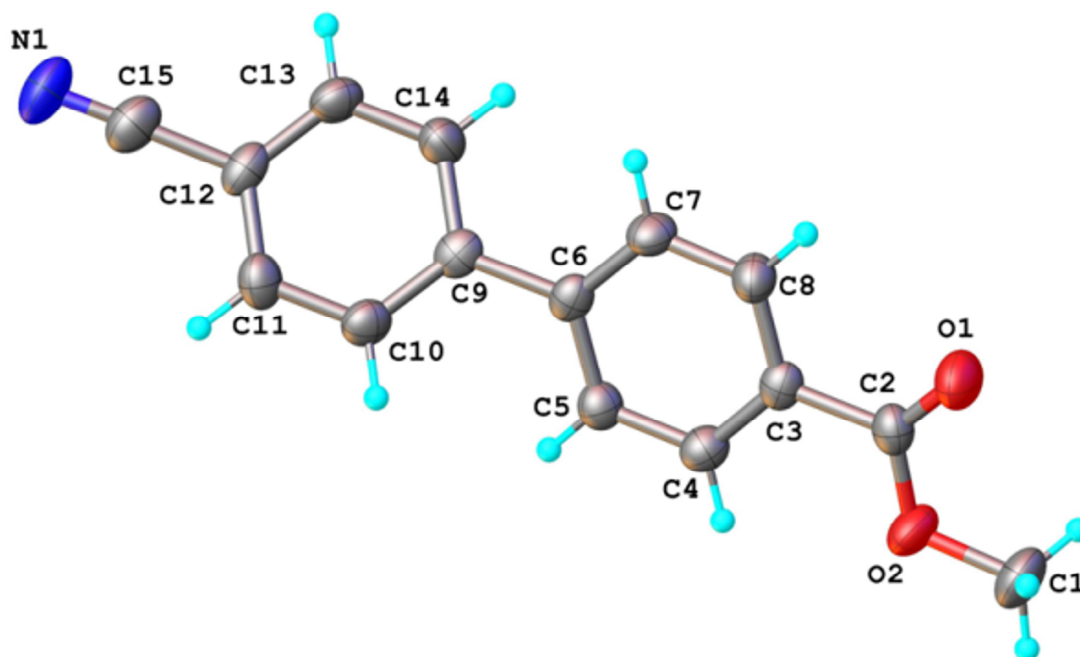


**Figure 3.** X-ray molecular structure of **5** (molecule **A**) with atom numbering and thermal ellipsoids at 50% probability level.

The molecular associates **1·2DMF** are assembled in the crystal into one-dimensional zig-zag supramolecular architectures by  $\pi$ - $\pi$  stacking interactions between tetrazole and biphenyl rings of adjacent entities, with a perpendicular distance of 3.459(3) Å and centroid-to-centroid distance of 3.8478(4) Å. A view of the supramolecular chain is shown in Figure 4. As shown in Figure 5, the crystal structure is built from the parallel packing of discrete 1D chains  $\{\mathbf{1}\cdot\mathbf{2DMF}\}_n$  along *b* crystallographic axis.

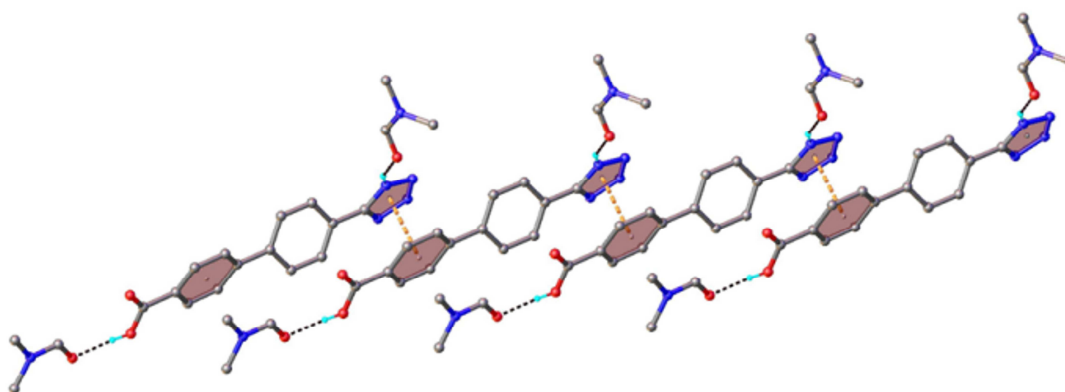


**Figure 4.** One-dimensional supramolecular architecture in **1·2DMF**. H-bonds and centroid-to-centroid distances are drawn in black and orange dashed lines, respectively. Non-relevant H-atoms are omitted for clarity.

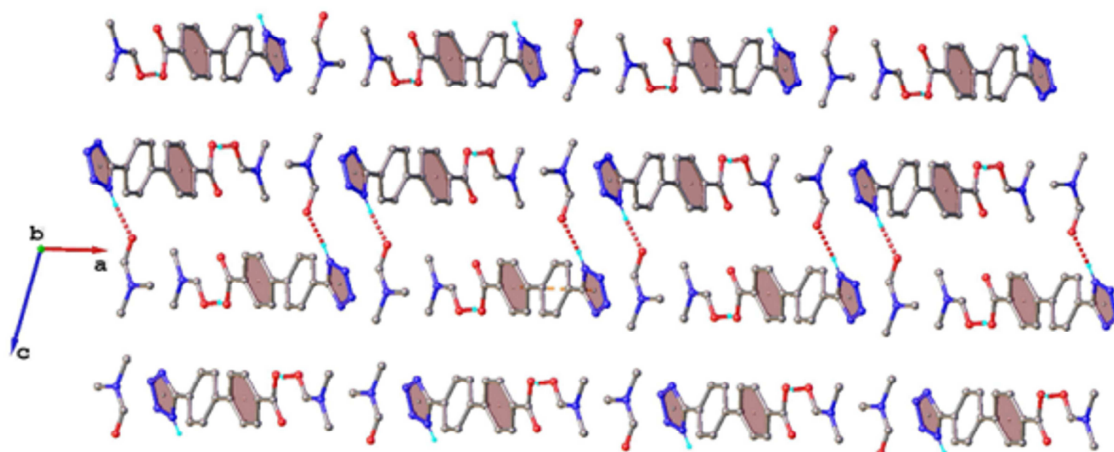


**Figure 5.** Packing diagram for **1·2DMF** viewed along *b* axis.

Due to the presence of aromatic rings in the molecules of **1**, **4** and **5**, the packing of these compounds shows common features, based on  $\pi$ - $\pi$  and C-H $\cdots$  $\pi$  interactions. A partial view of the crystal structure for compound **4** is presented in Figure 6. Compared to **1·2DMF**, the driving forces in the packing of **4** are determined by an extended system of C-H $\cdots$  $\pi$  contacts involving all aromatic rings. As a result, the main crystal structure motif can be characterized as a three-dimensional supramolecular architecture.

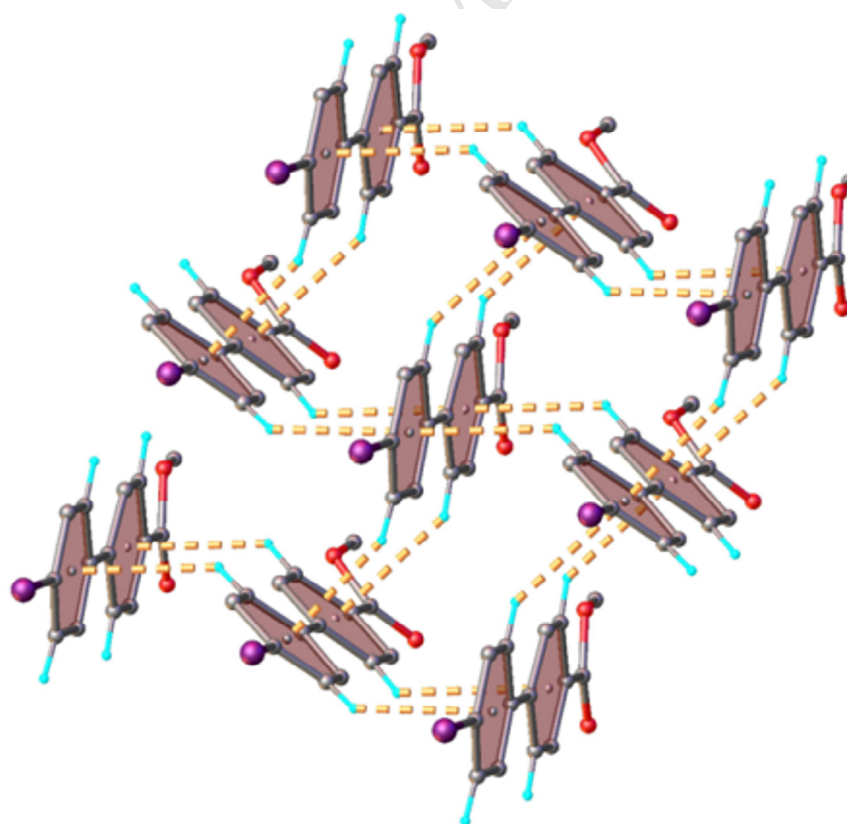


**Figure 6.** Partial view of 3D supramolecular network in the crystal structure **4**. Non-relevant H-atoms are omitted. C-H $\cdots$  $\pi$  contacts are in the range of 2.714÷2.962 Å.

In the crystal of **5**, the neutral entities **A** and **B** are arranged separately by  $\pi$ - $\pi$  interactions to form supramolecular ribbons of parallel stacked molecules, as shown in Figure 7. The centroid-to-centroid distances are equal to 3.912 Å, being the same for both ribbons, formed by **A** and **B** molecules. In the crystal, the self-assembled ribbons are arranged in parallel orientation along *a* crystallographic axis. A partial view of the packing diagram is presented in Supplementary Material (Figure S20).

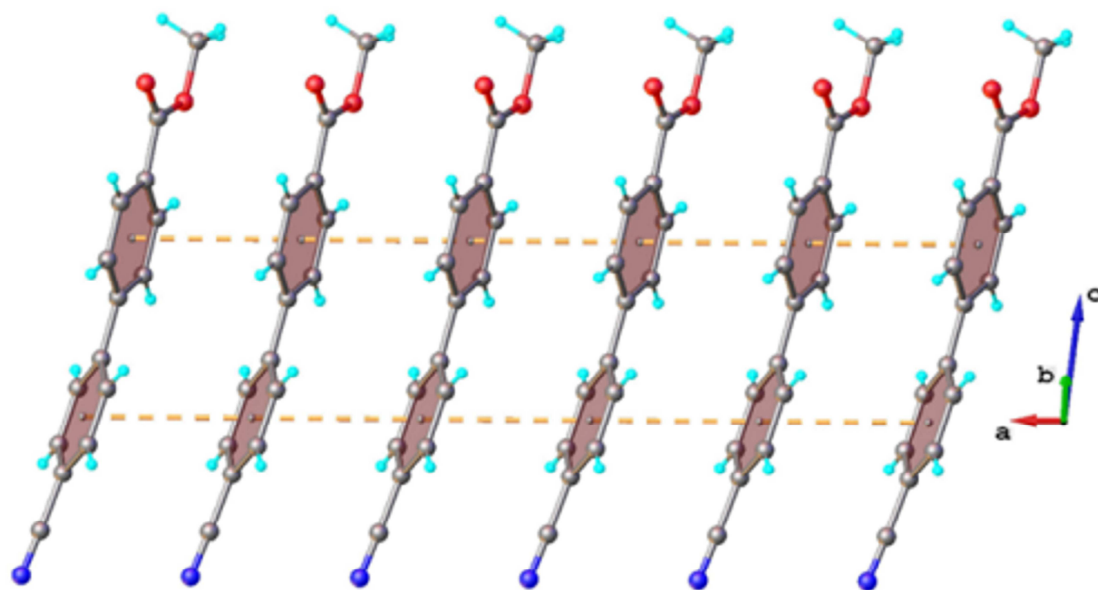


**Figure 7.**  $\pi$ - $\pi$  stacking in the crystal structure of compound **5**. Centroid-to-centroid distances are shown in dashed-orange lines.

### 3.5. Antimicrobial activity

To the best of our knowledge, available data on the antimicrobial activity of biphenylcarboxylic acids and their close structurally related derivatives is rather scarce. However, a brief inspection of the recent literature revealed a study that reported promising antimicrobial activities for a number of hydrazones of biphenylcarboxylic acid hydrazide [30]. In addition, a virtual screening, which was followed by experimental evaluations, established that four biphenylcarboxylic acids act as antivirulence agents against methicillin-resistant *S. aureus* by inhibiting the production of the toxins alpha-hemolysin and phenol-soluble modulins  $\alpha$  [31]. In an effort to gain insight into the biological activity of biphenylcarboxylic acids and esters, the compounds **1** and **3–6** reported in this study have been subjected to a preliminary *in vitro* antimicrobial susceptibility test against two reference strains of bacteria and one reference strain of yeast using the disk diffusion method.

Unfortunately, none of the tested compounds showed any inhibition of microbial growth against these three strains at concentrations up to 5 mg/mL. Although compounds **1** and **3–6** could yet exhibit weak antimicrobial activity at higher concentrations, this direction has not been pursued any further.

#### 4. Conclusions

4'-(2*H*-Tetrazol-5-yl)-[1,1'-biphenyl]-4-carboxylic acid, a valuable organic ligand for the synthesis of metal-organic frameworks, has been obtained through two distinct synthetic approaches. The first approach leads in five steps to the target compound in a very good yield of 68%, whereas the second approach affords to the same compound in two steps in 62% yield. Both approaches are amenable to scale-up, and can provide access to grams of the target compounds in a single batch. The structures of the target compound and of all the intermediates have been established using FT-IR and NMR spectroscopy. The solid state structure of the target compound **1** and intermediates **4** and **5** have been determined by single crystal X-ray diffraction method. The molecular associates **1·2DMF** form one-dimensional zig-zag supramolecular architectures by  $\pi$ - $\pi$  stacking interactions between tetrazole and biphenyl rings of adjacent entities. The main crystal structure motif of **4** can be characterized as a three-dimensional supramolecular architecture. The crystal of **5** is formed by supramolecular ribbons of parallel stacked molecules. The evaluation of antibacterial activity of the target compound **1** and of intermediates **3–6** against two bacterial strains and one fungal strain has shown that these compounds are inactive at concentrations up to 5 mg/mL.

#### Acknowledgment

The financial support of European Social Fund for Regional Development, Competitiveness Operational Programme Axis 1 – Project “Novel Porous Coordination Polymers with Organic Ligands of Variable Length for Gas Storage”, POCPOLIG (ID P\_37\_707, Contract 67/08.09.2016, cod MySMIS: 104810) is gratefully acknowledged.

#### Supplementary material

Spectroscopic data related to this article, the view of the packing diagram in **5** along *a* axis and information on the bond distances and angles in the crystals of compounds **1·2DMF**, **4** and **5** can be found at <http://xxxxxxxxxxx>. Crystallography data for compounds **1·2DMF**, **4** and **5** has been deposited with the Cambridge Crystallographic Centre. The data can be

obtained free of charge from CDCC, 12 Union Road, Cambridge CB2 1EZ, UK, Fax (+44) 1223-336-033, email: deposit@cdcc.cam.ac.uk or <http://www.ccdc.cam.ac.uk/getstructures>.

## References

- [1] H.W. Langmi, J. Ren, B. North, M. Mathe, D. Bessarabov, Hydrogen storage in metal-organic frameworks: A review, *Electrochim. Acta* 128 (2014) 368–392.
- [2] Y. Lin, C. Kong, Q. Zhang, L. Chen, Metal-organic frameworks for carbon dioxide capture and methane storage, *Adv. Energy Mater.* 7 (2017) 1601296.
- [3] H. Li, K. Wang, Y. Sun, C. T. Lollar, J. Li, H.C. Zhou, Recent advances in gas storage and separation using metal–organic frameworks, *Mater. Today* 21 (2018) 108–121.
- [4] X. Yang, Q. Xu, Bimetallic metal–organic frameworks for gas storage and separation, *Cryst. Growth Des.* 17 (2017) 1450–1455.
- [5] F. Jeremias, D. Fröhlich, C. Janiak, S. K. Henninger, Water and methanol adsorption on MOFs for cycling heat transformation processes, *New J. Chem.* 38 (2014) 1846–1852.
- [6] Y.B. Huang, J. Liang, X.S. Wang, R. Cao, Multifunctional metal–organic framework catalysts: synergistic catalysis and tandem reactions, *Chem. Soc. Rev.* 46 (2017) 126–157.
- [7] L. Zhu, X.Q. Liu, H.L. Jiang, L.B. Sun, Metal-organic frameworks for heterogeneous basic catalysis, *Chem. Rev.* 117 (2017) 8129–8176.
- [8] M. Dincă, A. Dailly, Y. Liu, C.M. Brown, D.A. Neumann, J.R. Long, Hydrogen storage in a microporous metal–organic framework with exposed Mn<sup>2+</sup> coordination sites, *J. Am. Chem. Soc.* 128 (2006) 16876–16883.
- [9] K. Sumida, M.L. Foo, S. Horike, J.R. Long, Synthesis and structural flexibility of a series of copper (II) azolate-based metal–organic frameworks, *Eur. J. Inorg. Chem.* (2010) 3739–3744.
- [10] H. He, Y. Song, F. Sun, N. Zhao, G. Zhu, Sorption properties and nitroaromatic explosives sensing based on two isostructural metal–organic frameworks, *Cryst. Growth Des.* 15 (2015) 2033–2038.
- [11] Q. Li, M.H. Yu, J. Xu, A.L. Li, T.L. Hu, X.H. Bua, Two new metal–organic frameworks based on tetrazole–heterocyclic ligands accompanied by *in situ* ligand formation, *Dalton Trans.* 46 (2017) 3223–3228.
- [12] H. He, F. Sun, H. Su, J. Jia, Q. Li, G. Zhu, Syntheses, structures and luminescence properties of three metal–organic frameworks based on 5-(4-(2*H*-tetrazol-5-yl)phenoxy)isophthalic acid, *CrystEngComm* 16 (2014) 339–343.

- [13] X. Wang, Q. Song, Y. Pan, S. Qiu, M. Xue, Two new cadmium metal-organic frameworks based on a mixed-donor ligand, *Chem. Res. Chin. Univ.* 32 (2016) 539–544.
- [14] A.J. Calahorro, G. Zaragoza, A.S. Castillo, J.M. Seco, A. Rodríguez-Diéguez, Unique metal-organic-framework with based on 4'-tetrazolate-4-biphenyl carboxylate spacer: Blue-green photoluminescence, *Polyhedron* 80 (2014) 228–232.
- [15] S.J. Bao, R. Krishna, Y.B. He, J.S. Qin, Z.M. Su, S.L. Li, W. Xie, D.Y. Du, W.W. He, S.R. Zhang, Y.Q. Lan, A stable metal–organic framework with suitable pore sizes and rich uncoordinated nitrogen atoms on the internal surface of micropores for highly efficient CO<sub>2</sub> capture, *J. Mater. Chem. A* 3 (2015) 7361–7367.
- [16] T.T. Li, Z.Z. Wen, S.L. Cai, S.R. Zheng, Construction of four d<sup>10</sup> coordination polymers containing binuclear rings as building blocks from 4'-(2*H*-tetrazol-5-yl)biphenyl-4-carboxylic acid, *J. Coord. Chem.* 69 (2016) 976–984.
- [17] P.J. Hajduk, M. Bures, J. Praestgaard, S.W. Fesik, Privileged molecules for protein binding identified from NMR-based screening, *J. Med. Chem.* 43 (2000) 3443–3447.
- [18] L. Costantino, D. Barlocco, Privileged structures as leads in medicinal chemistry, *Curr. Med. Chem.* 13 (2006) 65–85.
- [19] Z.J. Jain, P. S. Gide, R.S. Kankate, Biphenyls and their derivatives as synthetically and pharmacologically important aromatic structural moieties, *Arab. J. Chem.* 10 (2017) S2051–S2066.
- [20] C. Heering, B. Francis, B. Nateghi, G. Makhloufi, S. Lüdeke, C. Janiak, Syntheses, structures and properties of group 12 element (Zn, Cd, Hg) coordination polymers with a mixed-functional phosphonate-biphenyl-carboxylate linker, *CrystEngComm* 18 (2016) 5209–5223.
- [21] CrysAlisRED, Oxford Diffraction Ltd., Version 1.171.34.76, 2003.
- [22] O.V. Dolomanov, L.J. Bourhis, R.J. Gildea, J.A.K. Howard, H. Puschmann, OLEX2: a complete structure solution, refinement and analysis program, *J. Appl. Cryst.* 42 (2009) 339–341.
- [23] G.M. Sheldrick, SHELXS, *Acta Cryst. A* 64 (2008) 112–122.
- [24] E. Matuschek, D.F.J. Brown, G. Kahlmeter, Development of the EUCAST disk diffusion antimicrobial susceptibility testing method and its implementation in routine microbiology laboratories, *Clin. Microbiol. Infect.* 20 (2014) O255–O266.
- [25] Q. Wen, J. Jin, L. Zhang, Y. Luo, P. Lu, Y. Wang, Copper-mediated cyanation reactions, *Tetrahedron Lett.* 55 (2014) 1271–1280.

- [26] Y. Zhou, C. Yao, R. Ni, G. Yang, Amine salt-catalyzed synthesis of 5-substituted 1*H*-tetrazoles from nitriles, *Synth. Commun.* 40 (2010) 2624–2632.
- [27] I. Boldog, K.V. Domasevitch, J. Sanchiz, P. Mayer, C. Janiak, 1,3,5,7-Tetrakis(tetrazol-5-yl)-adamantane: The smallest tetrahedral tetrazole-functionalized ligand and its complexes formed by reaction with anhydrous  $M(II)Cl_2$  ( $M = Mn, Cu, Zn, Cd$ ), *Dalton Trans.* 43 (2014) 12590–12605.
- [28] F.F. Fleming, G. We, Cyclohexanecarbonitriles: Assigning configurations at quaternary centers from  $^{13}C$  NMR CN chemical shifts, *J. Org. Chem.* 74 (2009) 3551–3553.
- [29] R.J. Abraham, M. Reid, Proton chemical shifts in NMR. Part 15–Proton chemical shifts in nitriles and the electric field and  $\pi$ -electron effects of the cyano group, *Magn. Reson. Chem.* 38 (2000) 570–579.
- [30] A. Deep, S. Jain, P.C. Sharma, P. Verma, M. Kumar, C.P. Dora, Design and biological evaluation of biphenyl-4-carboxylic acid hydrazide-hydrazone for antimicrobial activity, *Acta Pol. Pharm.* 67 (2010) 255–259.
- [31] V. Khodaverdian, M. Pesho, B. Truitt, L. Bollinger, P. Patel, S. Nithianantham, G. Yu, E. Delaney, E. Jankowsky, M. Shoham, Discovery of antivirulence agents against methicillin-resistant *Staphylococcus aureus*, *Antimicrob. Agents Chemother.* 57 (2013) 3645–3652.

**Highlights**

- Synthesis of the title compound has been performed through two distinct approaches.
- Structural characterization has been performed using IR and NMR spectroscopy.
- Single crystal X-ray structures have been determined for two intermediates.
- Single crystal X-ray structure has been established for the title compound.
- Preliminary antimicrobial activity of the compounds has been evaluated.

ACCEPTED MANUSCRIPT